Chapter 4
ANALYTICAL TOOLS

BACKGROUND

In order to evaluate the data collected a number of definitions and analytical tools are required. The purpose of this chapter is to assemble this information for use in subsequent data analysis. The discussion which follows is an elaboration and application of some of the concepts introduced in Chapter 1.

ATMOSPHERIC EXTINCTION

Figure 4.1 illustrates in schematic form the atmospheric extinction of an incident beam due to scattering and absorption by air molecules and aerosol particles. Note that the total loss of beam intensity dI_λ at a particular wavelength λ when radiation passes through a medium of thickness dz can be expressed as the sum of several terms. A simplifying assumption which can often be made is that the aerosol particles only possess a real refractive index

$$m = m_R + i\, m_I \qquad \textbf{(4.1)}$$

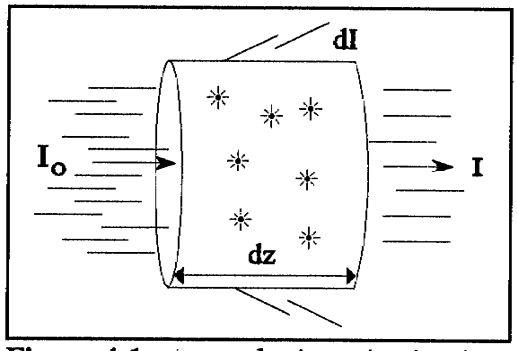

Figure 4.1: *Atmospheric extinction is due to scattering and absorption by molecules and aerosol particles.*

(i.e. that absorption is negligible) and that the radiation wavelength does not coincide with a CO_2 or water vapor absorption band. Under these assumptions the total intensity loss dI_λ as radiation passes through a layer dz can be written:

$$dI_\lambda = dI_{R\lambda} + dI_{O\lambda} + dI_{N\lambda} + dI_{P\lambda} = -(\alpha_{R\lambda} + \alpha_{O\lambda} + \alpha_{N\lambda} + \alpha_{P\lambda})\cdot I_{0\lambda}\, dz \qquad \textbf{(4.2)}$$

where $\alpha_\lambda = \alpha_{R\lambda} + \alpha_{O\lambda} + \alpha_{N\lambda} + \alpha_{P\lambda}$ is the total atmospheric *extinction coefficient*, $\alpha_{R\lambda}$ is the extinction coefficient due to molecular (Rayleigh) scattering, $\alpha_{O\lambda}$ and $\alpha_{N\lambda}$ are due to ozone and NO_2 respectively, and $\alpha_{P\lambda}$ is the extinction coefficient due to aerosol scattering. Note that the Rayleigh scattering term is due primarily to gaseous atmospheric oxygen and nitrogen, while extinction due to ozone and NO_2 occurs primarily in well-defined layers in the stratosphere.

For a given thickness dz the absolute value of $dI_\lambda/I_{0\lambda} = -\alpha_\lambda \cdot dz$ corresponds to the probability that a photon in the beam will be scattered from it when passing through the thickness dz. Integration of this differential equation leads to the familiar *Lambert-Beers' attenuation law*:

$$I_\lambda(z) = I_{0\lambda} \cdot \exp[-(\alpha_{R\lambda} + \alpha_{O\lambda} + \alpha_{N\lambda} + \alpha_{P\lambda})\cdot z] = I_{0\lambda} \cdot \exp(-\alpha_\lambda \cdot z) \qquad \textbf{(4.3)}$$

SCALE HEIGHT AND OPTICAL DEPTH

The quantity z is the "depth" of the atmosphere, an elusive quantity because the density of the atmosphere falls off as an exponential function of height. In a simplified model it is convenient to define a *scale height* H_p and to assume that the atmosphere extending to this altitude is uniform.

Another useful concept is the *air mass* M illustrated in Figure 4.2. Unit air mass $M = 1$ would correspond to the situation when radiation is vertically incident upon the atmosphere. In this case the *optical depth* τ can be introduced instead of the extinction coefficient as shown in Equation 4.4. From this result it is apparent that the optical depth $\tau = \alpha \cdot H_p$. Note that just as extinction coefficients are additive when various atmospheric constituents are being considered, so are atmospheric optical depths.

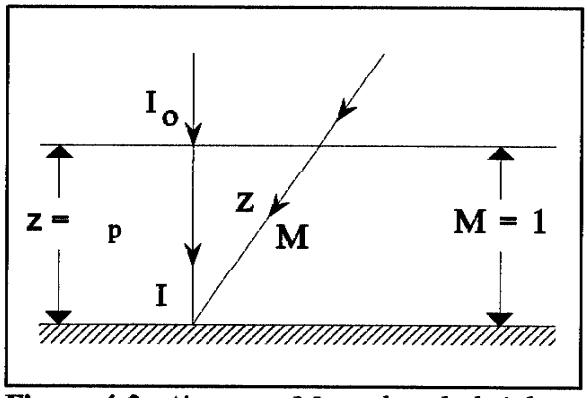

Figure 4.2: *Air mass* M *and scale height* H_p *are useful parameters.*

$$\frac{M}{1} = \frac{z}{H_p} \quad <=> \quad z = H_p \cdot M \quad thus \quad I = I_0 \cdot e^{-\alpha \cdot H_p \cdot M} = I_0 \cdot e^{-\tau \cdot M} \qquad (4.4)$$

We can now express the scattering probability for a photon passing through a layer of atmosphere of thickness dz as follows:

$$\frac{|dI|}{I} = \alpha \cdot dz = \frac{\tau \cdot dz}{H_p} \qquad (4.5)$$

Or using the second expression in Equation 4.4:

$$\frac{|dI|}{I} = \tau \cdot dM \qquad (4.6)$$

When written in this form it is apparent that the optical depth can be interpreted as the probability that a photon will be scattered during its passage through a given air mass interval dM. Assuming that the dominant extinction process is single scattering (neglecting multiple scattering is a reasonable assumption in view of the calculated mean free path of ca. 87 kilometers for a 550 nm photon in a clear atmosphere [*Chapter 1, p 7*]), the optical depth of a given component can be interpreted as *the probability that a photon in the direct solar beam will be scattered.*

AIR MASS CORRECTIONS

The air mass M which appears in Equation 4.4 will be closely approximated by $1/\cos \theta_Z$ where θ_Z is the solar zenith angle, provided the solar zenith angle does not exceed 60° [*Russell, 1993*]. For the large zenith angles commonly experienced in the Arctic, however, it becomes quite important to correct the air mass for the curvature of the Earth and to correct for refraction due to the vertical structure of

the atmosphere. This matter has been addressed in detail by Fritz Kasten and Andrew Young [*Kasten, 1989; Young 1994*] and others. The following algorithm provides a convenient and accurate method for computation of the Rayleigh air mass m_R as a function of the *true solar zenith angle* θ_Z:

$$m_R = \frac{1.002432\ \cos^2\theta_Z + 0.148386\ \cos\theta_Z + 0.0096467}{\cos^3\theta_Z + 0.149864\ \cos^2\theta_Z + 0.0102963\ \cos\theta_Z + 0.000303978} \quad (4.7)$$

The true solar zenith angle is available from well-known algorithms when the time and the geographical location are known, so that Young's equation for m_R can be readily incorporated into data handling routines.

Because the ozone and NO_2 layers are at an altitude of 20-30 kilometers the air mass for these atmospheric components will be slightly less than the Rayleigh air mass as given by Equation 4.7. For an observer at elevation h_O the air mass can be expressed as

$$\frac{R_E + h_L}{\sqrt{(R_E+h_L)^2 - (R_E+h_O)^2 \cdot \sin^2\theta_z}} \quad (4.8)$$

where θ_Z is the solar zenith angle, R_E is the Earth's radius, and h_L is the elevation of the layer of interest [*Komhyr, 1989*].

DIRECT BEAM IRRADIANCE

As mentioned in Chapter 1 the solar extraterrestrial irradiance I_0 varies during the year due to slight variations in the distance from the Earth to the Sun. N is the day of the year (note that the Earth is closest to the Sun on January 3rd). Thus I_0 can be expressed by

$$I_o = I_{sc} \cdot [1 + 0.033 \cdot \cos(2\pi\ \{N-3\}/365)] \quad (4.9)$$

where $I_{SC} = 1367\ W/m^2$ is the currently accepted value for the solar constant [*Beckman, 1991, p 6*]. The solar *spectral* irradiance $I_0(\lambda)$ will of course be subject to the same correction factor, so that the direct solar beam irradiance reaching the entry aperture of a pyrheliometer can be expressed as:

$$I(\lambda) = I_0(\lambda) \cdot e^{-\sum_i m_i(\theta_Z, z_{obs}) \cdot \tau_i(\lambda)} \quad (4.10)$$

with the exponent consisting of $m_R \cdot \tau_R(\lambda) + m_O \cdot \tau_O(\lambda) + m_N \cdot \tau_N(\lambda) + m_P \cdot \tau_P(\lambda)$ and corresponding to Rayleigh, ozone, NO_2 and aerosol extinction respectively. Note that in general the air mass is dependent upon the solar elevation angle as well as the altitude of the observer z_{obs}.

As we have seen in Chapter 3, *Instrumentation*, the data collected consists of pyrheliometer output signals $V(\lambda)$ for the wavelengths of interest with the instruments designed to provide linear response: $V(\lambda) = C \cdot I(\lambda)$. On this assumption we can

rewrite Equation 4.10 as:

$$V(\lambda) = V_0'(\lambda) \cdot e^{-\sum_i m_i \cdot \tau_i} \tag{4.11}$$

where $V_0'(\lambda)$ is the channel voltage which would be read at the top of the atmosphere at the current Earth-Sun distance. Equation 4.11 can be rearranged to yield an expression for the aerosol optical depth τ_P which is the physical quantity we want to reveal:

$$\tau_P = \frac{1}{m_P} \cdot [\ln V_0'(\lambda) - \ln V(\lambda) - m_R \tau_R - m_O \tau_O - m_N \tau_N] \tag{4.12}$$

Following [*Russell, 1993*] we define $V_P(\lambda)$ as the voltage which would be measured if aerosols were the only attenuator:

$$V_P(\lambda) = V(\lambda) \cdot e^{+m_R \tau_R(\lambda) + m_O \tau_O(\lambda) + m_N \tau_N(\lambda)} \tag{4.13}$$

whereby Equation 4.12 can be rewritten as:

$$\tau_P(\lambda) = \frac{1}{m_P} \cdot [\ln V_0'(\lambda) - \ln V_P(\lambda)] \tag{4.14}$$

If all quantities in Equation 4.13 are known (i.e. the measured value $V(\lambda)$ plus Rayleigh, ozone and NO_2 optical depths and air masses), then $V_P(\lambda)$ can be computed. If the top of the atmosphere voltage $V_0'(\lambda)$ is also known, e.g. from a Langley plot, then momentary values of the aerosol optical depth $\tau_P(\lambda)$ can be computed from Equation 4.14 or 4.12. The methods employed for determination of Rayleigh, ozone and NO_2 optical depths as well as corrections for temperature variations and changes in atmospheric pressure are described in Chapter 6.

Solving Equation 4.14 for $ln\ V_P(\lambda)$ as a function of τ_P yields the following useful relationship:

$$\ln V_P = \ln V_0'(\lambda) - \tau_P(\lambda) \cdot m_P \tag{4.15}$$

The equation shows that for periods of observation during which the aerosol optical depth at a given wavelength is constant, plotting $ln\ V_P(\lambda)$ against the aerosol air mass factor m_P should yield a straight line graph with a slope of $-\tau_P(\lambda)$. This important result is the heart of the technique we have used to determine the aerosol optical depths reported in our data presentation.

The uncertainties associated with this measurement technique have been evaluated in some detail by [*Russell, 1993*]. Experimental measurements using various apertures to assess the effect of diffuse light have been performed and are reported in connection with the description of instrumentation in Chapter 3.

AEROSOL PARTICLE SIZE

Having described the process required to find aerosol optical depths $\tau(\lambda)$, we describe in the following the analysis required in order to determine the aerosol particle size distribution $n(r)$. In this connection we will use some important quantities presented previously: the *aerosol size parameter* x and the *scattering efficiency factor* $Q_{ext}(x,m)$, where m is the *index of refraction* of the particle.

Aerosol size parameter

The *size parameter* x is given by:

$$= \frac{2\pi \cdot r}{\lambda} \qquad (4.16)$$

where r is the *radius* of a spherical particle, and λ is the *wavelength* of the incident radiation. The size parameter is the ratio of the circumference of the particle to the wavelength.

Extinction efficiency factor

The *extinction efficiency factor* Q_{ext} describes the scattering power of a molecule or an aerosol. For a spherical object with a diameter substantially larger than the wavelength diffraction effects can be neglected, the scattering cross section corresponds simply to the geometrical cross sectional area $\pi \cdot r^2$, and $Q_{ext} = 1$. For much smaller (sub-millimeter) particles light will be scattered from the beam due to diffraction even when it passes outside the geometrical cross section.

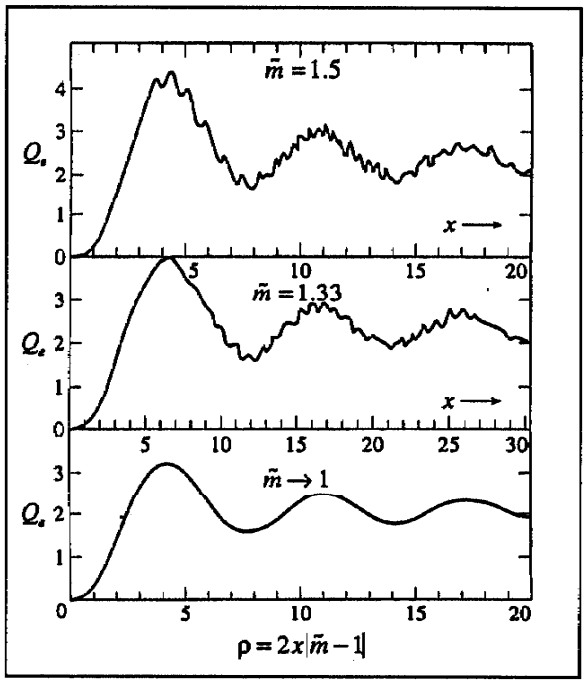

Figure 4.3: *This classic illustration due to van de Hulst shows scattering efficiencies of large dielectric spheres* [van de Hulst, 1957].

From physical optics it can be shown that for large particles with significant diffraction effects Q_{ext} approaches the value of 2. As particle sizes are further reduced (to tens of microns and less) the incident radiation interacts in a complex manner, and results like those shown in Figure 4.3 are observed. The effective cross section is then given by $Q_{ext} \cdot \pi \cdot r^2$ where knowledge of the functional form of Q_{ext} can be obtained from the Mie theory or by means of approximation methods such as van de Hulst's theory of anomalous dispersion [*Chapter 1, p 10*].

This theory yields the following approximation to the scattering efficiency factor:

$$Q_{ext}(\rho) = 2 - \frac{4}{\rho} \cdot \sin\rho + \frac{4}{\rho^2} \cdot (1 - \cos\rho) \qquad (4.17)$$

with Q_{ext} expressed here as a function of the *normalized size parameter* ρ defined as follows:

$$\rho = 2x \cdot (m-1) = \frac{2\pi \cdot d}{\lambda} \cdot (m-1) \qquad (4.18)$$

Note that Q_{ext} depends through this variable on the three fundamental scattering parameters: *wavelength* λ, the *particle radius* r and the *refractive index* m of the particle. Using the size parameter $x = 2\pi r/\lambda$ allows us to write $Q_{ext}(x,m)$.

It is this scattering efficiency factor which is displayed in the lower panel of Figure 4.3. Although the theory fails to reproduce the fine structure shown by the Mie theory, this is often unimportant in atmospheric applications because of the mixture of sizes occurring in natural aerosols.

The wavy structure visible for larger values of x (and thus of ρ) in Figure 4.3 is due to interference between the light which is transmitted through the particles and the light diffracted around them. Notice that the separation $\Delta\rho$ between successive extrema is about 2π. For large values of x ($\rho > 10$) Q_{ext} no longer varies so much, implying that scattering for this range of particle sizes is not strongly dependent on wavelength (so clouds with micron-size particles appear white).

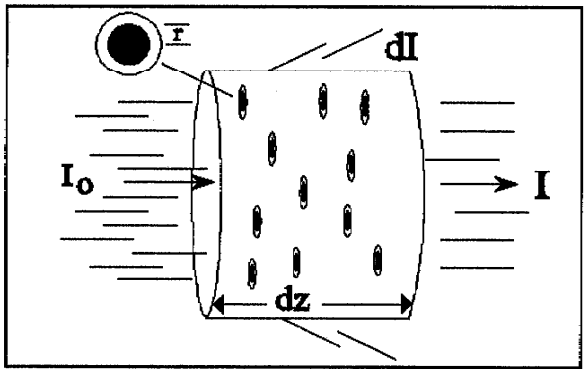

Figure 4.1: *Scattering centers with effective cross sections* $Q_{ext}\pi \cdot r^2$ *due to diffraction.*

Consider scattering from a beam of radiation of cross sectional area A. Figure 4.4 shows how scattering centers with effective cross sectional areas $Q_{ext} \cdot \pi \cdot r^2$ scatter radiation from a beam passing through a medium with thickness dz. Now assume that the particle density N_0 in this medium is such that it is unlikely that the particles will occlude one another. The chance of scattering for the incident photons can then be expressed as follows:

$$\frac{|dI|}{I} = \frac{\pi r^2 \cdot Q_{ext} \cdot N_0 \cdot A \cdot dz}{A} = \pi r^2 \cdot Q_{ext} \cdot N_0 \cdot dz \qquad (4.19)$$

The numerator in the middle expression in this equation corresponds to the effective scattering area $\pi r^2 \cdot Q_{ext}$ of each particle multiplied by the particle density N_0 and the volume $A \cdot dz$ of the beam segment, i.e. by the number of particles. The denominator is the total beam area A. Thus the ratio is the *effective scattering area* divided by the *total area*.

So far we have assumed that we are dealing with particles of uniform radius r. If the distribution of particle sizes is characterized by a dimensionless function $n(r)$, then the probability of scattering for a beam passing through dz becomes:

$$\frac{|dI|}{I} = dz \cdot \int_0^\infty \pi r^2 \cdot Q_{ext} \cdot N_0 \cdot n(r)\ dr \qquad (4.20)$$

Equating this result with the previous expression for the scattering probability from Equation 4.5 yields:

$$\frac{|dI|}{I} = \frac{\tau \cdot dz}{H_p} = dz \cdot \int_0^\infty \pi r^2 \cdot Q_{ext} \cdot N_0 \cdot n(r)\ dr \qquad (4.21)$$

$$\tau = H_p \cdot N_0 \int_0^\infty \pi r^2 \cdot Q_{ext} \cdot n(r)\ dr \qquad (4.22)$$

It is this relationship between the aerosol optical depth and the size distribution which is often cited in the literature and taken as the starting point for an analysis of the optical detection of the aerosol particle size distribution *n(r)*.

The task of extracting *n(r)* from Equation 4.22 involves the solution of a *Fredholm integral equation*. A detailed description this mathematical problem and how it is solved has been and continues to be a subject of considerable interest in the literature of atmospheric physics [*Twomey, 1962; Quenzel, 1970; Kaufman, 1994; Nakajima, 1983, 1986; Amato, 1996; Box, 1996; Shifrin, 1996*]. S. Twomey's book on the mathematics of inversion in remote sensing offers a highly recommended comprehensive treatment [*Twomey, 1977*].

The essence of the problem is as follows. We have the following optical depth data available from our measurements:

wavelength	λ_1	λ_2	. . .	λ_N
aerosol optical depth	$\tau_{\lambda 1}$	$\tau_{\lambda 2}$	. . .	$\tau_{\lambda N}$

Table 4.1: *The optical depth data available for further analysis has the structure shown here.*

In the usual solution strategy the functional form of the unknown function *n(r)* is assumed, and the function includes *N* fitting parameters. A set of variational equations must be formed and reduced to a set of *N x N* equations using the method of residuals to find new values of the fitting parameters. The goodness of fit is checked using Equation 4.22, and iteration is continued until the value of the integral matches the observed values of τ as closely as possible at all of the measured wavelengths (or the solution diverges). This generalized least squares method is described in standard textbooks of mathematical analysis [*Press, 1988*]. An overview of the inversion algorithm used in this work is shown in Figure 4.5 on the following page.

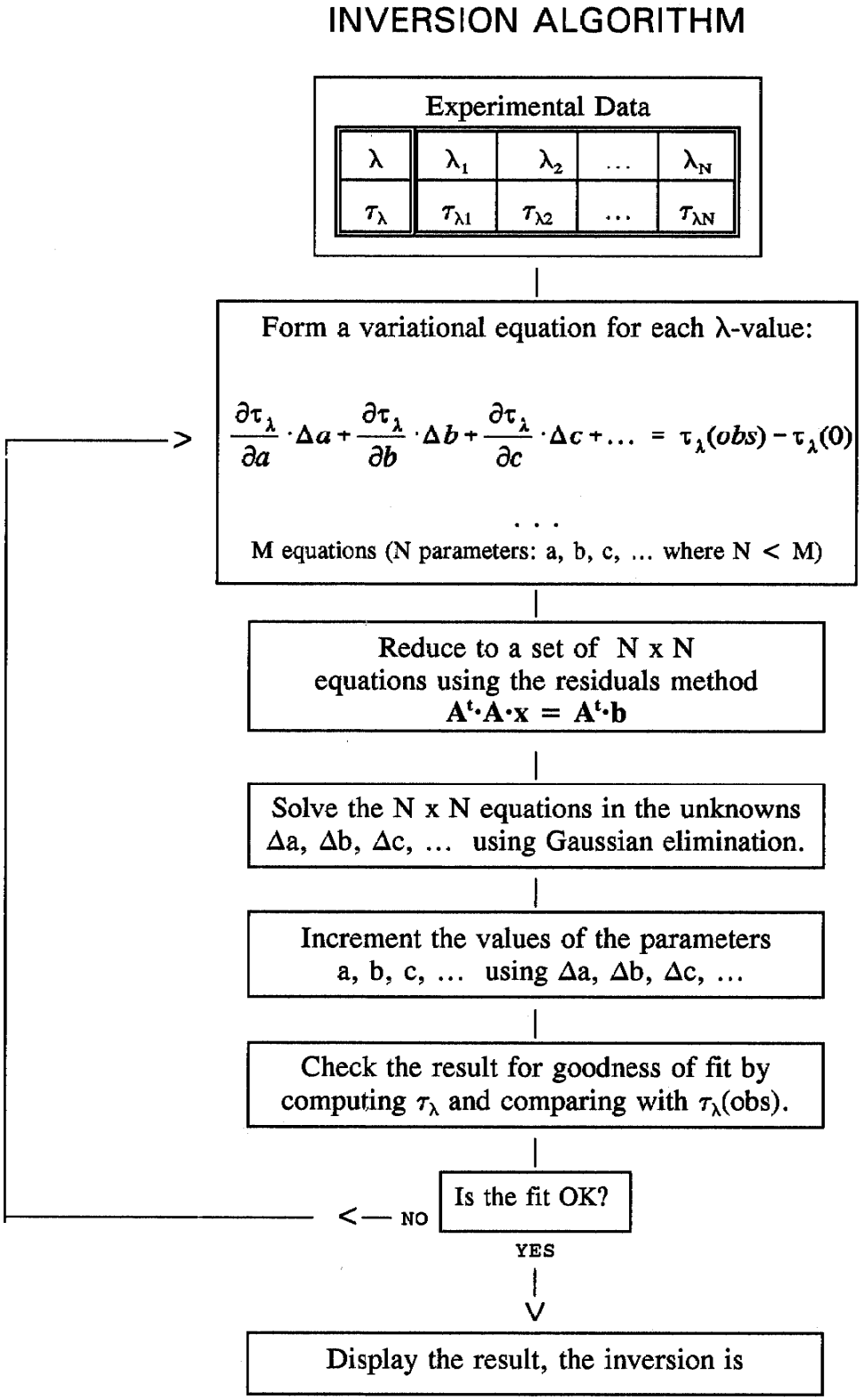

Figure 4.5: *Overview of the inversion algorithm used in this work to find particle size distributions.*

PARTICLE SIZE DISTRIBUTIONS

It is helpful to consider various reasonable options for the particle size distribution function $n(r)$ which might be used to analyze data and at the same time to establish an intuitive feeling for the physical meaning of the equation

$$\tau_\lambda = H_p \cdot N_0 \int_0^\infty \pi r^2 \cdot Q_{ext} \cdot n(r)\ dr \qquad (4.23)$$

This knowledge is essential in order to make a plausible choice for the proposed function $n(r)$ to match a given set of optical depth data $\{(\lambda_i,\tau_i)\}$. No matter what function one may choose to apply, a normalization requirement must be fulfilled, so that the integral over all particle sizes yields the correct value for the particle number in the atmospheric column.

With respect to units we recall that the scale height H_p has the units of length, and that the mean particle number density N_0 has the units of reciprocal volume. The product $H_p \cdot N_0$ can therefore be interpreted as the mean number of particles per unit area in a column up to the "top" of the atmosphere. To insure consistency with units care must be exercised when interpreting the meaning of the size distribution function. The particle radius value r when it appears in $n(r)$ can be interpreted as a dimensionless parameter, and the units μm^{-1} can be associated with $n(r)$. If the integral is taken over a particle size range measured in microns, so that dr has the units μm and $n(r)$ has the units μm^{-1}, then $n(r) \cdot dr$ represents the fraction of all particles in the column having radii in the range from r to $r+dr$.

$$\int_0^\infty H_p \cdot N_0 \cdot n(r)\ dr = H_p \cdot N_0 \qquad (4.24)$$

Having stated this *normalization requirement*, let us review a variety of aerosol size distribution functions which might be contemplated.

MONORADIAL DISTRIBUTION

Suppose that all particles in the aerosol have the same radius r_0. In this case a delta function $\delta(r - r_0)$ is a good choice for $n(r)$:

$$\int_0^\infty H_p \cdot N_0 \cdot \delta(r - r_0)\ dr = H_p \cdot N_0 \qquad (4.25)$$

It is immediately clear that this function satisfies the normalization requirement due to the properties of the delta function. What would Equation 4.23 then predict about the optical depth τ_λ?

$$\tau_\lambda = H_p \cdot N_0 \int_0^\infty \pi \cdot r^2 \cdot Q_{ext} \cdot \delta(r - r_0)\ dr \qquad (4.26)$$

With a constant particle radius r_0 the integral can be reduced to:

$$\tau_\lambda = H_p \cdot N_0 \cdot \pi \cdot r_0^2 \cdot Q_{ext} \qquad (4.27)$$

The factor $H_p \cdot N_0$ is the number of particles in the column per unit area, and the

factor $\pi r_0^2 \cdot Q(x_0,m)$ is the scattering cross section of each particle. For low particle densities the product is the total scattering probability for this wavelength and particle size. Quickly considering a numerical example: Aitken particles at the South Pole with a uniform radius $r = 0.10\ \mu m$ are reported to yield an aerosol optical depth $\tau_\lambda = 0.012$ at $\lambda = 500$ nm [*Shaw, 1982*]. What number concentration and total column aerosol burden would this correspond to? The scattering efficiency $Q_{ext} \approx 2$ for the assumed particle radius as can be seen from Figure 4.6 (derived from Equation 4.17).

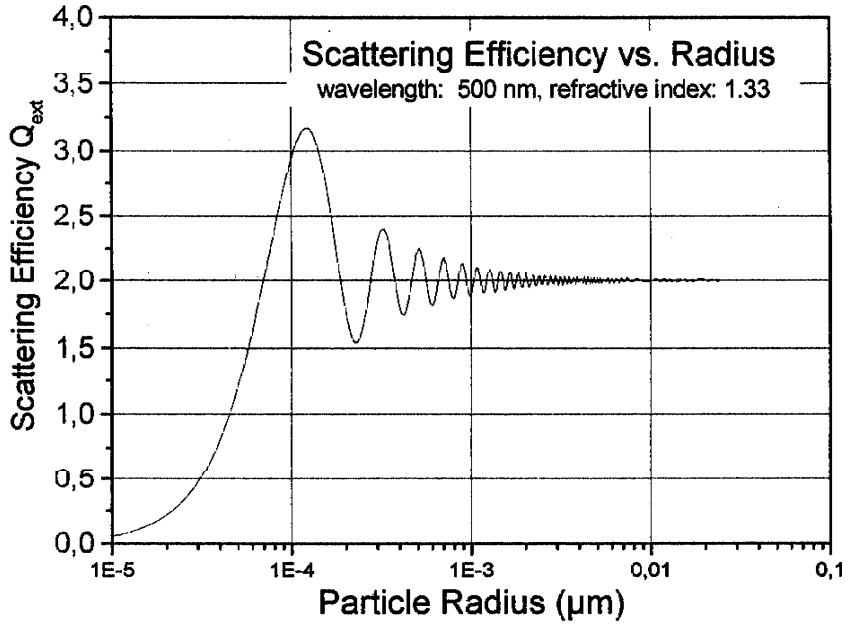

Figure 4.6: *The scattering efficiency factor Q_{ea} is shown for $\lambda = 500$ nm and $m = 1.33$ (water).*

Solving for the particle density yields the result $N_o \approx 24\ cm^{-3}$ with a scale height $H_p = 8$ km. Assuming that the density of the individual particle is about $1\ g/cm^3$, the total column content in this case would be less than $0.1\ \mu g$. A comparable value for an urban environment with 10.000 particles/cm^3 would be about $35\ \mu g$. For low particle concentrations and single scattering, we have shown in Chapter 1, Equation 1.8, that the mean free path ℓ of a photon equals the reciprocal of the extinction coefficient α. In this example $\alpha \approx 1.5 \cdot 10^{-5}\ cm^{-1}$ and the mean free path due to aerosol scattering would be over 600 km. In the urban environment with high aerosol concentrations the photon mean free path due to aerosol would be about 1.5 km, and visibility would be severely reduced.

NORMALLY DISTRIBUTED PARTICLE SIZES

Having considered a particularly simple case with aerosol particles of uniform size, let us examine the situation when the mean aerosol radius equals r_0 and the standard deviation of the normal distribution of particle sizes is s_0. Such a distribution has a number of useful properties, and it is sometimes encountered in the case of fresh aerosol where settling has not yet caused removal of the largest particles. For

factor $\pi r_0^2 \cdot Q(x_0,m)$ is the scattering cross section of each particle. For low particle densities the product is the total scattering probability for this wavelength and particle size. Quickly considering a numerical example: Aitken particles at the South Pole with a uniform radius $r = 0.10\ \mu m$ are reported to yield an aerosol optical depth $\tau_\lambda = 0.012$ at $\lambda = 500$ nm [*Shaw, 1982*]. What number concentration and total column aerosol burden would this correspond to? The scattering efficiency $Q_{ext} \approx 2$ for the assumed particle radius as can be seen from Figure 4.6 (derived from Equation 4.17).

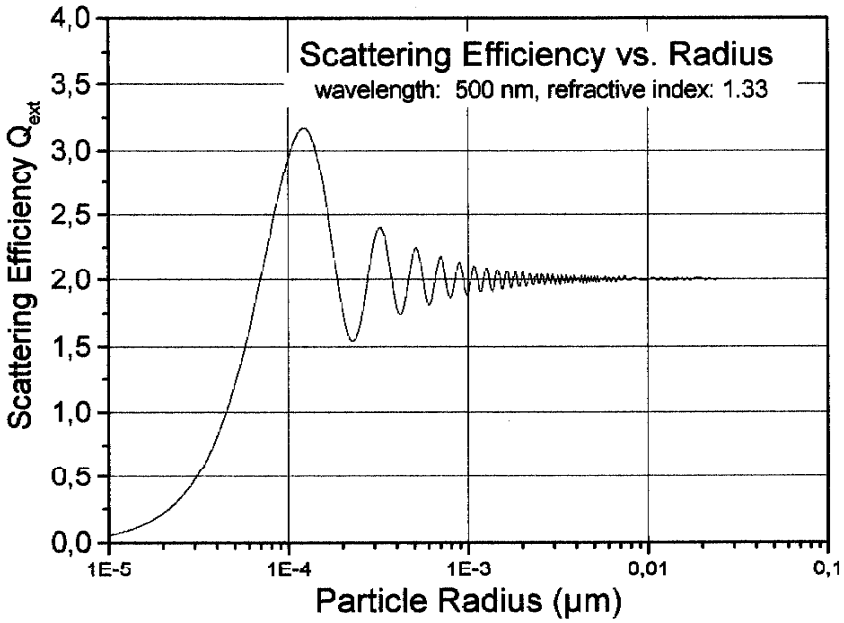

Figure 4.6: *The scattering efficiency factor Q_{ext} is shown for $\lambda = 500$ nm and $m = 1.33$ (water).*

Solving for the particle density yields the result $N_o \approx 24\ cm^{-3}$ with a scale height $H_p = 8$ km. Assuming that the density of the individual particle is about $1\ g/cm^3$, the total column content in this case would be less than $0.1\ \mu g$. A comparable value for an urban environment with 10.000 particles/cm^3 would be about $35\ \mu g$. For low particle concentrations and single scattering, we have shown in Chapter 1, Equation 1.8, that the mean free path ℓ of a photon equals the reciprocal of the extinction coefficient α. In this example $\alpha \approx 1.5 \cdot 10^{-8}\ cm^{-1}$ and the mean free path due to aerosol scattering would be over 600 km. In the urban environment with high aerosol concentrations the photon mean free path due to aerosol would be about 1.5 km, and visibility would be severely reduced.

NORMALLY DISTRIBUTED PARTICLE SIZES

Having considered a particularly simple case with aerosol particles of uniform size, let us examine the situation when the mean aerosol radius equals r_0 and the standard deviation of the normal distribution of particle sizes is s_0. Such a distribution has a number of useful properties, and it is sometimes encountered in the case of fresh aerosol where settling has not yet caused removal of the largest particles. For

clarity we begin with the simplest case, a *monomodal normal distribution* function:

$$H_p \cdot N_0 \cdot n(r) = \frac{H_p \cdot N_0}{s_0 \sqrt{2\pi}} e^{-\frac{1}{2}\left(\frac{r-r_0}{s_0}\right)^2} \tag{4.28}$$

checking the normalization requirement

$$\int_0^\infty H_p \cdot N_0 \cdot n(r)\, dr = \frac{H_p \cdot N_0}{s_0 \sqrt{2\pi}} \int_0^\infty e^{-\frac{1}{2}\left(\frac{r-r_0}{s_0}\right)^2} dr \tag{4.29}$$

Changing variables in the integral to $t = (r - r_0)/s_0$ with $dt = dr/s_0$ we can rewrite the integral (noting that the limits will change from "0 to ∞" with the old variable to "$-\infty$ to ∞" with the new variable):

$$\int_0^\infty H_p \cdot N_0 \cdot n(r)\, dr = \frac{H_p \cdot N_0}{s_0 \sqrt{2\pi}} \int_{-\infty}^{\infty} e^{-\frac{1}{2}t^2} s_0\, dt \tag{4.30}$$

The infinite integral evaluates to $\sqrt{2\pi}$, so the normalization condition is indeed fulfilled:

$$\int_0^\infty H_p \cdot N_0 \cdot n(r)\, dr = H_p \cdot N_0 \tag{4.31}$$

Figure 4.7 shows a graph of such a particle distribution function. Note that it can be completely characterized by the three parameters: (N_0, r_0, s_0).

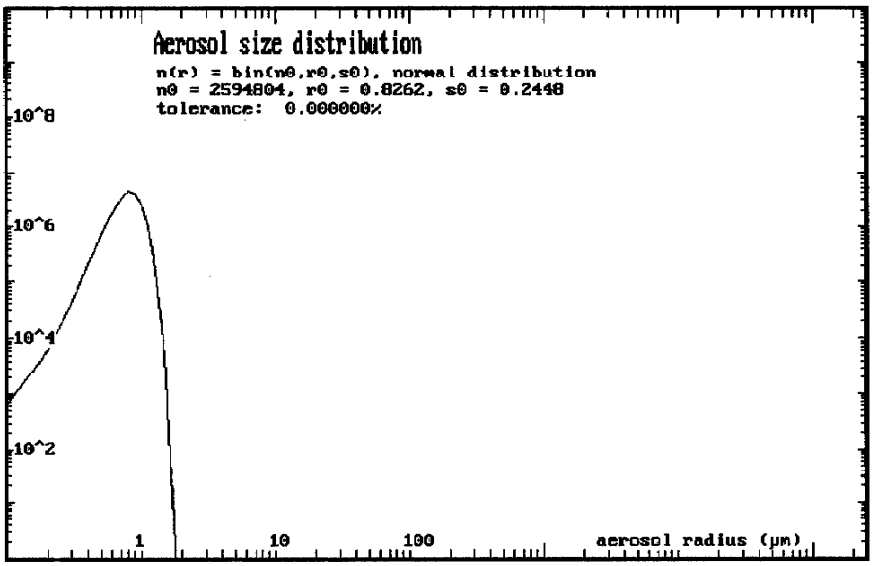

Figure 4.7: *A monomodal normal aerosol particle size distribution extracted from the aerosol integral equation using Quenzel's optical depth data.*

Wavelength (nm)	400	500	600	700	800	900	1000	1500
Optical Depth τ	0.078	0.079	0.090	0.107	0.117	0.121	0.121	0.090

Table 4.2: *Published aerosol optical depth data taken from measurements by H. Quenzel* [Quenzel, 1970, p 2920] *at the Equator (30°W) on September 29th, 1965.*

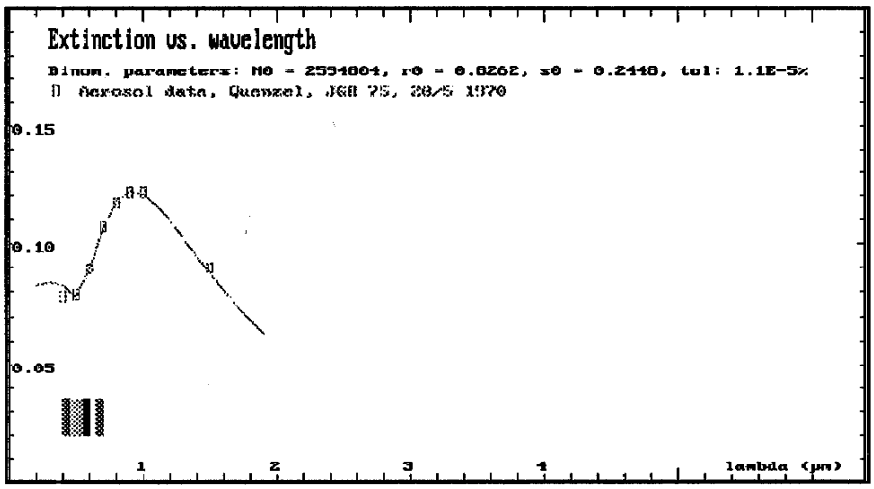

Figure 4.8: *Extinction vs. wavelength measured by H. Quenzel at the Equator (30°W) on September 29th, 1965.*

The fitting graph shown here was found using the algorithm described in Figure 4.5 using a monomodal normal distribution to describe the aerosol size distribution. Examination of Figure 4.8 shows that this distribution function provides excellent accord with Quenzel's data. It was found that the fitting process was quite critical with respect to the choice of initial parameters. The program AER-INVX.CML therefore includes an option for experimenting with a number of possible parameter sets to check the fit before setting the automatic fitting routine of Figure 4.5 into operation.

Considerations similar to the case of the monomodal binomial distribution can be applied to the bimodal distribution:

$$H_p \cdot N_0 \cdot n(r) = \frac{H_p \cdot N_1}{s_1\sqrt{2\pi}}\, e^{-\frac{1}{2}\left(\frac{r-r_1}{s_1}\right)^2} + \frac{H_p \cdot N_2}{s_2\sqrt{2\pi}}\, e^{-\frac{1}{2}\left(\frac{r-r_2}{s_2}\right)^2} \qquad (4.32)$$

This assumption is often more realistic, because there are usually far more small particles than large ones, a fact which is not reflected in the assumption of a monomodal distribution. The bimodal model provides for two normally distributed groups of particles: N_1 in the small radius range (0.01-0.50 μm) and N_2 in the large radius range ($>$ 0.50 μm). In this case a total of six parameters must be found: three (N_1,r_1,s_1) describing the small-particle normal distribution and three (N_2,r_2,s_2) describing the large-particle distribution. Although the bimodal hypothesis is often more realistic than the monomodal, considerable experimentation may be required to find reasonable initial values which will lead to convergence.

POWER LAW SIZE DISTRIBUTIONS

Because experience has shown that there are far more small particles than large particles, it is tempting to use a power law function to describe the distribution. Some sample data from the literature is shown in Table 4.3 with typical aerosol optical depth data after corrections have been made for Rayleigh scattering and ozone absorption.

Wavelength (nm)	369	500	675	776	862	1048
Optical Depth τ	0.137	0.109	0.089	0.080	0.074	0.065

Table 4.3: *Typical published aerosol optical depth data in the visible and NIR spectral regions from Dalu, Rao, et al.* [Dalu, 1995] *showing data from Southern Sardinia.*

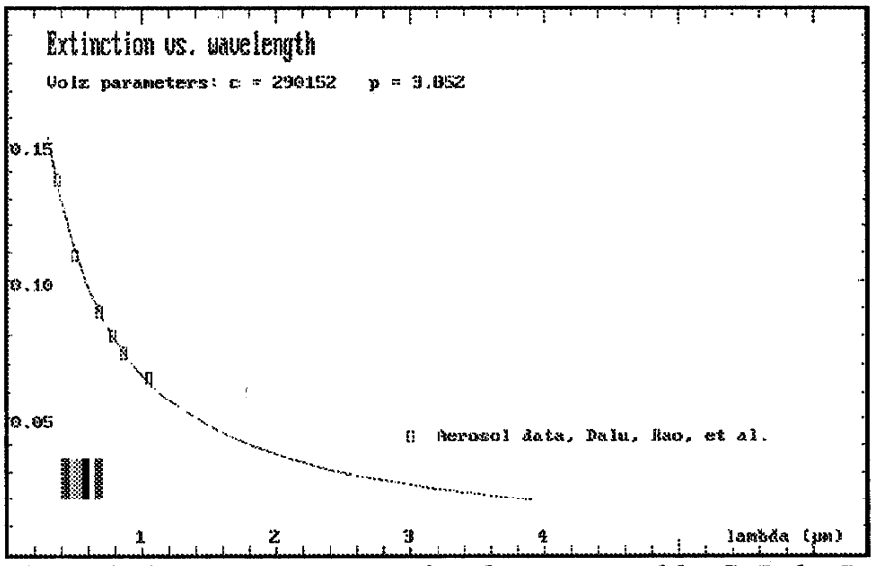

Figure 4.10: *Extinction vs. wavelength as measured by G. Dalu, R. Rao, et al. in early summer of 1995 in Southern Sardinia.*

The power law function to describe $n(r)$ in this case has the functional form

$$n(r) = C \cdot r^{-p} \tag{4.33}$$

In order to satisfy the normalization requirement, Equation 4.24, it is necessary to limit the range to $[r_1; r_2]$, and it turns out that the constant C must fulfill:

$$C = \left[\frac{1-p}{r_2^{1-p} - r_1^{1-p}} \right] \tag{4.34}$$

This is dependent on the size range selected and does not have clear physical meaning. Some authors warn about the limitations of the power law distribution [*Seinfeld, 1998, p 426*]. Nevertheless the power law distribution is used extensively in the literature to describe aerosol size distributions. The algorithm of Figure 4.5 was used to fit the data of Dalu, et al. in Figure 4.10 to a power law distribution, and it is a useful tool in spite of its limitations.

SUMMARY

In this chapter we have reviewed some of the basic definitions and analytical tools which can be directly applied to the analysis of our data from Thule Air Base. The definition of aerosol optical depth and its relationship to Rayleigh, ozone and NO_2 optical depths should be noted and in particular Equation 4.15 which plays an important role in the interpretation of our data.

The inversion algorithm for extracting the aerosol size distribution function from aerosol optical depth data has been described and its practical application to analyze data from the literature has been demonstrated. After a brief presentation of the measurements acquired at Thule Air Base in Chapter 5, we will proceed in Chapter 6 to analyze the optical depth data which we have measured.